

Table 2
Assignment of the infrared bands for PANi and Pt/PANi.

Band (cm^{-1})		Assignment
PANi	Pt/PANi	
786	795	Aromatic C–H bending of the aniline ring [41]
1114	1113	N=Q=N/in-plane deformation of (C–H), Q=NH ⁺ –B [42,43]
1275 $\nu(\text{C–N}^{*})$ in the polaron lattice of PANi [44]	1288 $\nu(\text{C–N})$ of secondary aromatic amine [45,46]	Aromatic C–N stretching of the aniline unit
1468	1472	C=C stretching of aromatic ring [42,47]
2150	2167	Water (bending vibration)
2682	2631	O–H stretching
	3109	Aromatic C–H stretch
3437	3410	Adsorbed water symmetric stretching, bending [48]
3958	3869	Aromatic C–H stretching [42,43,47]

Q: Quinonoid ring; B: Benzenoid ring.

platinum, the changes of much importance for this study are the following:

1. The stretching frequency, $\nu(\text{C–N}^{*})$ in the polaron lattice of PANi at 1275 cm^{-1} is altered to the stretching frequency, $\nu(\text{C–N})$ of secondary aromatic amine in PANi, indicating a decrease in the number of polarons in Pt/PANi thereby affecting the conductivity of the Pt/PANi.
2. The combined symmetric stretching and bending frequencies of adsorbed water at 3437 cm^{-1} in PANi, decreases in strength on inclusion of Pt. The extent of the presence of adsorbed water is reduced by the presence of metallic platinum which could influence the hydrogen bonding between free water and the polymer matrix and hence facilitate water drain.

The conductivity of PANi, calculated from the resistivity measured by the four-probe method was found to be $1.055 \text{ mho cm}^{-1}$, while that of Pt/PANi composite was measured to be $0.764 \text{ mho cm}^{-1}$. The decrease in the conductivity of Pt/PANi is attributed to the decrease in the number of polarons due to the reduction of Pt(IV) on the PANi matrix which affects the oxidation state of PANi and hence its conductivity. The decrease in the number of polarons is also indicated by the IR spectra. This is not a concern for the use of Pt/PANi in the cathode interlayer as the H^{+} furnished by weakly ionized water molecule and those which reach from the anode side will restore the optimum conductivity of PANi in the operating conditions of PEMFC.

The cyclic voltammograms (CV) of PANi and Pt/PANi, recorded in $0.1 \text{ M H}_2\text{SO}_4$ solution are shown in Fig. 11. In order to simulate the conditions of the operating fuel cell, we used a larger area of

the working electrode (0.6132 cm^2) compared with the usual CV electrode, and observed a current density much higher than that of platinum electrode used in the usual CV studies. A small bump corresponding to the hydrogen reduction was observed at about -0.2 V vs Ag/AgCl in the case of PANi (Fig. 11a and b). CV patterns of Pt/PANi show oxygen reduction shoulder at about $0.6\text{--}0.7 \text{ V}$. In all the four cases (Fig. 11a–d) the reversible adsorption and desorption of the respective gases (N_2 and O_2) could be observed in the low current regions. These CV curves (Fig. 11) show that PANi and Pt/PANi can be used as the electrode material in PEMFC without involving any additional electrochemical reactions of their own. While the PANi electrode showed varying capacitive current on adsorption of nitrogen and oxygen, Pt/PANi registered almost similar CVs (Fig. 11c and d) highlighting its usefulness as the electrode material for electrochemical reactions. Also, the sensitivity of Pt/PANi (in terms of current density) is high when compared to that of PANi only. Both PANi and Pt/PANi showed electrostatic capacitance with the polymer as the micro electrodes and the gas (O_2) as the dielectric. This is in tune with the effective-medium-type dielectric function expected for a granular metallic system [49]. The capacitive behaviour indicates the double-layer formation at the interface [50]. This capacitance can facilitate the electrochemical reaction on the catalyst layer with ease, as a part of the activation energy is gained in the interlayer itself. The schematic diagram of the activation energy of the fuel cell in the presence of Pt/PANi interlayer can be illustrated as in Fig. 12. The double layer capacitance enhances the energy of the oxidant by 'a' as shown in Fig. 12, and hence the electrochemical reaction has a lesser energy requirement ($=b - a$).

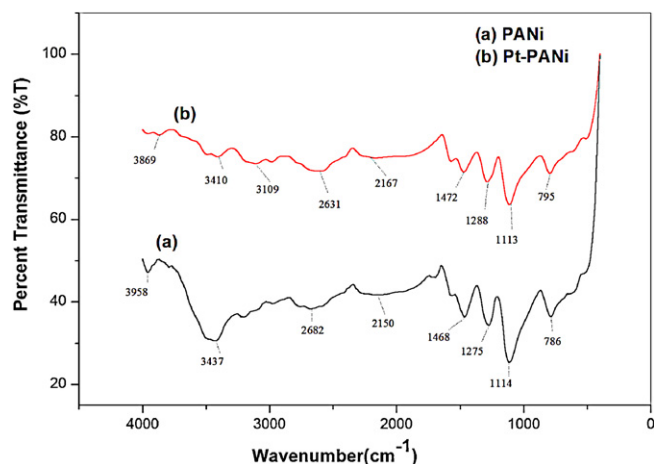


Fig. 10. Infrared spectra of (a) PANi (b) Pt-PANi.

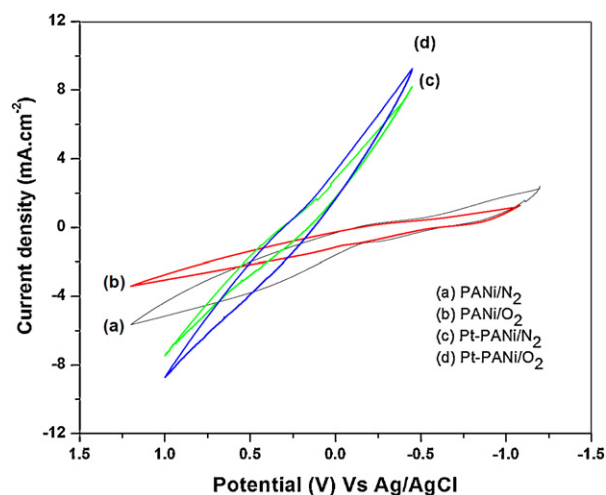


Fig. 11. Cyclic voltammograms of PANi and Pt-PANi in $0.1 \text{ M H}_2\text{SO}_4$: (a) PANi/ N_2 , (b) PANi/ O_2 , (c) Pt-PANi/ N_2 and (d) Pt-PANi/ O_2 .